**Running title:**

MATE-type citrate transporter in legume

**Corresponding Author:**

Kazufumi Yazaki

Laboratory of Plant Gene Expression, Research Institute for Sustainable Humanosphere,

Kyoto University, Gokasho, Uji 611-0011, Japan

Tel.: +81-774-38-3617 (extension: 3617)

Fax: +81-774-38-3623

E-mail: yazaki@rish.kyoto-u.ac.jp

**Subject Areas:**

Membrane and transport

**Number of black and white figures, color figures and tables:**

0, 8, 0, respectively

**Title:**

LjMATE1, a Citrate Transporter Responsible for Iron Supply to Nodule Infection Zone of *Lotus japonicus*.

**Authors:**

Kojiro Takanashi[1], Kengo Yokosho[2], Kazuhiko Saeki[3], Akifumi Sugiyama[1], Shusei Sato[4], Satoshi Tabata[4], Jian Feng Ma[2], Kazufumi Yazaki[1*]

**Authors Addresses:**

[1] Research Institute for Sustainable Humanosphere, Kyoto University, Gokasho, Uji 611-0011, Japan

[2] Research Institute for Bioresources, Okayama University, Kurashiki 710–0046, Japan

[3] Department of Biological Sciences, Faculty of Science, Nara Women's University, Nara, 850-6503 Japan

[4] Kazusa DNA Research Institute, 2-6-7 Kazusa-kamatari, Kisarazu, Chiba 292-0818, Japan

**Abbreviations:**

ARA, acetylene reduction activity; DAB, diaminobenzidine; dpi, days post inoculation; GUS, β-glucuronidase; ICP-MS, inductively coupled plasma mass spectrometry; MATE, multidrug and toxic compound extrusion; MBS, modified Barth's saline; NAS, nicotianamine synthase; pLjMATE1, *LjMATE1* promoter region; RNAi, RNA interference; SNF, symbiotic nitrogen fixation.

**Footnotes:**

AB649311: The nucleotide sequence reported in this paper has been submitted to DDBJ under accession numbers.

**Abstract:**

Symbiotic nitrogen fixation by intracellular rhizobia within legume root nodules requires the exchange of nutrients between host plant cells and their resident bacteria. While exchanged molecules imply nitrogen compounds, carbohydrate, and also various minerals, the knowledge on molecular basis of plant transporters that mediate those metabolite exchanges are still limited. In this study, we have shown that a multidrug and toxic compound extrusion (MATE) protein, LjMATE1, is specifically induced during nodule formation, which nearly paralleled the nodule maturation, in a model legume *Lotus japonicus*. Reporter gene experiments indicated that the expression of *LjMATE1* was restricted to the infection zone of nodules. To characterize the transport function of LjMATE1, we conducted biochemical analysis using heterologous expression system with *Xenopus* oocyte, and found that LjMATE1 is a specific transporter for citrate. Physiological roles of LjMATE1 was analyzed with RNA interference (RNAi) line, which revealed limited growth of RNAi line under nitrogen deficiency condition with inoculation of rhizobia compared to the control. It was noteworthy that, Fe localization was clearly altered in nodule tissues of RNAi line. These results strongly suggest that LjMATE1 is a nodule-specific transporter that assists the Fe translocation from the root to nodules by providing citrate.

**Key words:**

Citrate, Fe translocation, *Lotus japonicus*, MATE, nodulation,

## Introduction

Nitrogen-fixing symbiosis between legume plants and soil bacteria called rhizobia is one of the most important symbioses on the earth. They are not only a major source of fixed nitrogen in natural ecosystems, but also the single largest natural source of nitrogen for agriculture (Smil 1999). Symbiotic nitrogen fixation (SNF) in legumes takes place in specialized organs called nodules that develop from dedifferentiated root cells after infection by rhizobia in the soil in a species-specific manner. Via infection threads rhizobia colonize in developing nodule tissue (Brewin 1991) and ultimately they enter cortical cells by endocytosis (Verma and Hong 1996). This nodule development is accompanied by coordinated differentiation of both plant and bacterial cells, which results in forming both infected and uninfected plant cells, which are developed in a mosaic form. During nodulation, global change in gene expression was involved in both partners (Colebatch et al. 2004, Kouchi et al. 2004, Uchiumi et al. 2004). Many of these changes strongly affect both plant and bacterial metabolisms and transports, which become specialized for supporting the exchange of reduced carbon and other nutrients from the plant to bacteroids, and fixed nitrogen from the bacteroids to the plant (White et al. 2007). It is postulated that many transporters are involved in the exchange of these nutrients, and thus for several transporters have been identified, e.g. SST1, a symbiotic sulfate transporter in *Lotus japonicus* (Krusell et al. 2005) and an allantoin transporter, PvUPS1 in french bean (*Phaseolus vulgaris*) (Pelissier et al. 2004), but overall understandings of membrane transport systems in nodule are still very limited.

Multidrug and toxic compound extrusion (MATE) proteins widely occur in bacteria, fungi, mammals, and also in plants (Omote et al. 2006). Apparently plants have a higher diversity of

MATE-type transporters than bacteria and animals e.g., there are 56 MATE orthologs in *Arabidopsis thaliana*, while only two members are found in human genome. AtDTX1was the first identified plant MATE, which was isolated from the Arabidopsis cDNA library using a bacterial mutant defective in multidrug resistance (Li et al. 2002). AtDTX1 showed efflux activity for a variety of xenobiotics, however, further studies on other plant MATEs revealed that many of them showed rather restricted substrate specificity for their own metabolites such as flavonoids, alkaloids, and citrate. In particular, MATE-type transporters, which transport citrate, are reportedly involved in iron (Fe) translocation or aluminum (Al) detoxification in plants. For instance, FRD3 from Arabidopsis demonstrated as a citrate transporter is localized at the pericycle and cells internal to the pericycle cells in roots, and is required for Fe translocation from the roots to the shoots (Green and Rogers 2004, Durrett et al. 2007). Defects in this transporter resulted in the precipitation of Fe in the root vasculature (Green and Rogers 2004, Durrett et al. 2007). Also in monocots, a rice MATE transporter OsFRDL1, transports citrate at the pericycle cells of the roots, and was suggested to be involved in Fe translocation in the xylem as well (Yokosho et al. 2009). On the other hand, two studies have shown in 2007 that Al-induced secretion of citrate in barley (*Hordeum vulgare*) and sorghum (*Sorghum bicolor*) is mediated through MATE transporters (Furukawa et al. 2007, Magalhaes et al. 2007). Secretion of citrate from the roots is a mechanism of Al resistance in many plant species (Ma et al. 2001, Kochian et al. 2005, Delhaize et al. 2007). In addition, more recent studies have shown that two soybean MATE-type transporters, GmFRD3a and GmFRD3b, as well as ScFRDL1 from *Secale cereal* mediated Fe translocation (Rogers et al. 2009, Yokosho et al. 2010).

In order to comprehend the membrane transporters involved in SNF we have performed

transcriptome analysis following laser microdissection in a model legume *Lotus japonicus.* From this microarray experiments, a MATE-type transporter (*LjMATE1*) was identified as a nodule-specific gene in *L. japonicus* (Takanashi et al. 2012b). In this study, we demonstrate that LjMATE1 can transport citrate, and assist the translocation of Fe to nodule infection zone, which is essential to support nodule function.

## Results

### Expression analysis of *LjMATE1* during nodulation

Based on our microarray analysis in nodules of *L. japonicas,* a MATE-type transporter gene (*LjMATE1*) is suggested to be involved in nitrogen fixation in this plant due to the high expression in the infection zone. To confirm the *in silico* data experimentally, expression analysis was carried out. Using gene-specific primers we found that the expression of *LjMATE1* was specifically observed in nodules of *L. japonicus* (Fig. 1A). Time-course experiment at five different nodulation stages revealed that the gene expression of *LjMATE1* was dramatically increased at 7 days post inoculation (dpi) of *Mesorhizobium loti* and kept high level during SNF (Fig. 1B).

To analyze the tissue specific expression of *LjMATE1* in nodules in more detail, we isolated 1.7 kb fragment upstream of the translational initiation codon from *L. japonicus* genomic DNA, which contains the putative *LjMATE1* promoter region (*pLjMATE1*), and was fused to β -glucuronidase (GUS) reporter gene. The binary vector containing *pLjMATE1*::GUS reporter system was then introduced into *L. japonicus* with hairy root transformation method. GUS expression analysis clearly showed that *LjMATE1* was expressed only in nodules and no

expression was seen in root tissues through nodulation (Fig. 1C-H). To identify the cell type where *LjMATE1* is expressed, nodule sections were prepared after GUS staining. Microscopic observation revealed that the GUS staining was observed mainly in the infected cells of nodules at 7 and 21 dpi (Fig. 1D, F). While, GUS staining decreased in central infection zone at 35 dpi (Fig. 1H).

**LjMATE1 has transport activity for citrate**

Plant MATE proteins can be divided into two distinct groups by their amino acid sequences, which seems to reflect their transport substrate, i.e., citrate and others. LjMATE1 belongs to a clade, in which all reported citrate-transporting MATE proteins are clustered, with high amino acid sequence similarity with GmFRD3a (72%) and GmFRD3b (71%), which are involved in Fe translocation from root to aerial parts (Rogers et al. 2009) (Fig. 2). To evaluate if LjMATE1 has the activity to transport citrate as a substrate, we expressed LjMATE1 in *Xenopus* oocytes. Fig. 3 showed the transport assay using radioisotope-labeled citrate. The data indicated that the efflux activity for citrate was significantly higher in the oocytes pre-injected with LjMATE1 cRNA than in oocytes injected with water as a negative control. This efflux activity of LjMATE1 was almost the same with HvAACT1, a previously reported citrate-transporting MATE (Supplementary Fig. S1) (Furukawa et al. 2007). We also examined transport activity of malate, which is used as energy source in bacteroids (Price et al. 1987), however, oocytes pre-injected with LjMATE1 cRNA did not show specific transport activity for malate compared with control (Fig. 3).

**Growth phenotype of *LjMATE1* knockdown line**

To determine the physiological role of LjMATE1, we suppressed its expression in transgenic plants by RNA interference (RNAi). Among 20 stable transformants, appreciable suppression of *LjMATE1* expression was found in an RNAi line (*ljmate1*) at T2 generation (Fig. 4A). As control, we used other RNAi line (*LjMATE1*) in which *LjMATE1* gene expression was not suppressed in addition to wild-type. The T2 RNAi line grew normally with nitrogen nutrient supplementation, and no apparent phenotype difference was observed compared to the wild-type. While when plants were inoculated with *M. loti* under nitrogen deficiency condition, the RNAi plant showed clear growth defect phenotype (Fig. 4B, C), suggesting that the ability of SNF was reduced in the knockdown line. Then we observed nodule phenotype of the *ljmate1* line. Accompanied with normal pink nodules that were normally seen in control plants, about one third of nodules in *ljmate1* revealed greenish appearance (Fig. 5A-D). The nodule size of *ljmate1* was significantly smaller than that of control plants (Fig. 5E), and the acetylene reduction activity (ARA) of nitrogenase was also significantly reduced in *ljmate1* as well as the expression level of *leghemoglobin* (Fig. 5F, G).

**Fe accumulation in *LjMATE1* knockdown nodules**

MATE-type transporters, which have transport activity for citrate, are known to be involved in either Fe translocation or Al resistance. To investigate whether LjMATE1 mediates Fe translocation or not, Fe localization in nodules of RNAi plants was examined with Perls staining (Green and Rogers 2004). While visible Fe precipitation was not observed in control nodules (Fig. 6A, B), strong Perls staining was detected at root-nodule junction area and nodule vascular

bundle of RNAi nodules (Fig. 6C, D), indicating altered Fe localization in *ljmate1* nodules. This staining pattern was not observed in *LjMATE1* nodules (control) (Fig. 6E, F). To observe Fe localization in more detail with nodule sections, the iron staining was enhanced by second reaction with diaminobenzidine (DAB) and hydrogen peroxide (Roschzttardtz et al. 2009). Fig. 7A and 7B clearly showed that Fe was accumulated mainly in the infection zone of wild-type nodule, especially in infected cells, where a large amount of leghemoglobin is accumulated. It is to be noted that almost no Fe accumulation was observed in root vascular bundle of wild-type plant (Fig. 7C). In contrast, Fe localization in nodules of *ljmate1*was seen in infected cells, but the level was much low in particular in the central zone (Fig. 7D, E). Another clear difference was observed in the root vascular bundle of *ljmate1*, where high Fe deposition was detected (Fig. 7F). Fe accumulation pattern in the nodules of another control *LjMATE1* was almost the same with wild-type nodules (Fig. 7G-I).

For quantitative comparison, we determined Fe content in the nodules using inductively coupled plasma mass spectrometry (ICP-MS). The Fe content in the nodules of stable *ljmate1* was significantly lower compared to that in wild-type (decreased by 43.2%) (Fig. 8), and the contents of other metals, such as Zn and Mg, were not significantly changed between wild-type and *ljmate1* (Fig. 8). These results strongly suggested that LjMATE1 is involved in Fe translocation in nodules by releasing citrate, which is essential to support the function of SNF.

## Discussion

Fe storage is of a special importance in nodules, especially in infected cells, because of a high accumulation of leghemoglobin and nitrogenase, both of which requires Fe for their activity.

Several studies demonstrated a part of mechanisms of Fe accumulation in nodules. For instance, Fe (II) transport activity across peribacteroid membrane was measured in soybean nodules (Moreau et al. 1998), and later a transporter that mediates the Fe movement at peribacteroid was identified as GmDMT1 (Kaiser et al. 2003). Fe (III) is also provided across peribacteroid membrane when chelated with several organic acids such as citrate, and accumulates in the peribacteroid space, where Fe (III) reductase activity is present (LeVier et al. 1996). In contrast with Fe transport across peribacteroid membrane, the mechanisms of Fe translocation from root tissues to nodules, especially to infected cells, have been unknown. In this study, we characterized LjMATE1 and found that this MATE-type protein mediates Fe translocation into infected cells by releasing citrate into apoplast in infection zone.

Expression analysis by qPCR showed that *LjMATE1* expression was induced at 7 dpi and reached a maximum at 12 dpi (Fig. 1B). This induction pattern is similar to the expression of leghemoglobin and nitrogenase activity. Moreover, promoter analysis revealed that expression of *LjMATE1* was restricted to the infection zone of nodules, suggesting LjMATE1 is directly involved in SNF.

The physiological role of LjMATE1 was demonstrated by generating transgenic plants, in which the expression of *LjMATE1* was suppressed by RNAi. Previous reports on Fe deficient mutants in Arabidopsis frd3 and rice osfrdl1 showed chlorosis in cotyledons or leaves especially under low Fe condition (Durrett et al. 2007, Yokosho et al. 2009). However, the knockdown line *ljmate1* demonstrated in this study did not show such phenotype in nitrogen sufficient condition, as LjMATE1 functions exclusively in nodules as indicated in the expression analysis (Fig. 1A). When *ljmate1* plants were inoculated with rhizobia under nitrogen deficiency

condition, the growth was apparently suppressed compared to wild-type, but not with supplementation of nitrogen nutrient (Fig. 4C). In addition, *ljmate1* have many greenish nodules (Fig. 5B, D), which are known as inactive in SNF. Indeed, ARA of *ljmate1* nodules was significantly reduced (Fig. 5F), indicating that LjMATE1 is requires for SNF and suppression of *LjMATE1* caused fix- nodules.

DAB-enhanced Perls staining was first applied in plant tissue to detect Fe accumulation in Arabidopsis embryos, in which the staining was too weak by the single Perls staining alone (Roschzttardtz et al. 2009). In this study we have employed this DAB-enhancement to monitor the Fe accumulation in nodule sections. In wild-type nodules, Fe accumulation was detected mainly in the infection zone, which is consistent with the physiological functions of Fe in nodules (Fig. 7A, B). However, Fe staining was apparently fainted in the infection zone of *ljmate1* nodules particularly in the central region (Fig. 7D, E). Then, we determined Fe contents in nodules using ICP-MS, and found the reduced Fe concentration in *ljmate1* nodules (Fig. 8). These results strongly suggest the involvement of LjMATE1 in Fe accumulation in nodules by increasing Fe mobility.

Moreover, unusual Fe deposition was seen in the root vascular bundles in the *ljmate1* plant as well (Fig. 6D, 7F), which may be a secondary phenomenon of stagnant Fe delivery into the nodules, as the expression of *LjMATE1* is restricted to the infection zone of nodules (Fig. 1C-H). The spacial difference in tissues between the relevant gene expression and the Fe accumulation was also observed in rice (Kobayashi et al. 2010), i.e., rice OsYSL2 functioning as a transporter of Fe-nicotianamine complex is expressed mainly in the phloem cells of leaves and leaf sheaths, whereas the RNAi lines of OsYSL2 showed increased Fe accumulation in roots (Koike et al.

2004, Ishimaru et al. 2010).

Plants utilize highly sophisticated mechanisms for Fe uptake and translocation among organs. As naturally abundant $Fe^{3+}$ is hardly water-soluble, plants secrete various molecules to increase the Fe solubility, for instance, nicotianamine and citrate to form Fe-chelator complex (Conte and Walker 2011). The accumulation of nicotianamine in nodules has not been reported, however, Hakoyama and co-workers showed that a nicotianamine synthase (NAS) that mediated the reaction from *S*-adenosylmethionine to nicotianamine, was expressed in a late stage of nodulation in *L. japonicus*, and they postulated that LjNAS2 is involved in Fe reuse from inactive nodule to other organs (Hakoyama et al. 2009). It is reported that citrate, which also serves as chelator of Fe, accumulates in nodules, while the citrate content decreases to approximately 60% when plant is inoculated by ineffective *Rhizobium* (Rosendahl et al. 1990). In this study, we could not demonstrate the transport direction of citrate by LjMATE1, but we presume that LjMATE1 effluxes citrate at plasma membrane into apoplast by the following reasons. 1) Fe accumulation is decreased in the infected cells when *LjMATE1* expression was suppressed (Fig. 7 and 8); 2) Fe movement in peribacteroid space is possible without citrate, where Fe (III) -chelator complex can be reduced to Fe (II) and/or bound with siderophores released by the bacteroid (LeVier et al. 1996, Wittenberg et al. 1996). For the uptake of Fe-citrate complex into infected cells other metal transporters may be involved. In fact, metal transporter genes, such as Zrt/Irt-like protein (ZIP) and natural resistance-associated macrophage protein (Nramp), are up-regulated during nodulation in our transcriptomic analysis besides *LjMATE1* (Takanashi et al. 2012b). Detailed characterization of these transporters will enable us to grasp the overall scheme of Fe exchange between bacteroids and plant cells.

## Material and Methods

### Plant materials and growth conditions

*L. japonicus* MG-20 Miyakojima was used in this work. Seeds were surface-sterilized with a 1% sodium hypochloride solution for 10 min, rinsed five times with sterile distilled water, then germinated on water agar plate (0.8%). Five-day-old seedlings were transferred on sterile vermiculite with liquid 1/2 B&D medium (Broughton and Dilworth 1971) in plant box and grown in a cultivation chamber under a 16-h day/8-h night cycle at temperatures of 23°C.

### Expression analysis with rhizobia

To obtain RNA samples, 9-day-old seedlings were inoculated with *M. loti* MAFF303099, which was cultured overnight in TY medium at 28°C. For organ-specific expression analysis, plants at 19 dpi were sampled. Time course analysis was conducted by collecting aerial parts and underground parts respectively, at 0, 2, 4, 7, 12, and 19 dpi. Reverse transcription was carried out using a SuperscriptIII Reverse Transcriptase (Invitrogen), followed by semi-qPCR (95°C for 1 min, 32 cycles at 95°C for 20 s, 55°C for 30 s and 72°C for 20 s) using Go Taq DNA Polymarase (Promega) with the sets of primers specific to *LjMATE1* (forward primer, 5'-GCTACACAACCCATCAATGC-3' and reverse primer, 5'-TGCAAATGAGACCATCACCA-3'). *Ubiquitin* (forward primer, 5'-ATGCAGATCTTCGTCAAGACCTTGAC-3' and reverse primer, 5'-ACCTCCCCTCAGACGAAGGA-3') was used as an internal control. For qPCR (95°C for 15 min, 40 cycles at 94°C for 10 s, 56°C for 20 s and 72°C for 25 s), DyNAMO HS SYBR Green

qPCR Kit (Finnzymes) was used. Real-time detection of PCR products was performed using Roter-Gene 3000A (Corbett Research).

**Histochemical analysis of promorter-GUS transformant of *L. japonicus***

A fragment of 1.7 kb upstream the start codon of *LjMATE1* was amplified from genome DNA of MG-20 using Phusion High-Fidelity DNA Polymerase (Finnzymes) with a set of specific primers, forward primer, 5'-ACAAGTTTGTACAAAAAAGCAGGCTCTTGGAAGGGGCTGTCTTTT-3'; reverse primer, 5'-ACCACTTTGTACAAGAAAGCTGGGTGATATCCTAAATCTTATGTAA-3' (the underlined positions are non-native sequences of the *att*B recombination sites). The PCR product was subcloned into pDONR/Zeo (Invitrogen), and then transferred into a Gateway-compatible binary vector, pGWB3 (Nakagawa et al. 2007). The construct was then introduced into *L. japonicus* using hairy-root transformation mediated by *Agrobacterium rhizogenes* LBA1334, as previously reported (Kumagai and Kouchi 2003). The transformed plants were inoculated with *M. loti* and grown in a cultivation chamber under the condition mentioned above. Nodules were sampled at 7, 21, and 35 dpi, respectively, and GUS staining was performed as described previously (Takanashi et al. 2011)

**Transport assay in *Xenopus* oocytes**

The full-length cDNA of *LjMATE* was cloned into the oocyte vector pXβG-evl. The plasmid was linearized with *Sac*II, and cRNA was transcribed in vitro with T3 RNA polymerase (mMESSAGE mMACHINE kit; Ambion). Oocytes were isolated from adult female *Xenopus*

*laevis* frogs as described before (Ma et al. 2006). Selected oocytes were incubated for 1 day in modified Barth's saline (MBS) at 18°C until the injection of cRNA. A 50 nl of water solution containing 50 ng cRNA or not was injected into each oocyte with a nano-jector II (Drummond Scientific Company), followed by incubating in MBS at 18°C for 2 days. For determining citrate efflux activity, a 50 nl of 2.4 mM $^{14}$C-labeled citrate or malate (2.3 nCi/oocyte) was injected. The oocytes were then washed four times with MBS buffer (pH 7.6) and then transferred into a 500 µl of fresh buffer at 18°C. After 30 min incubation, the external buffer was sampled and the oocytes were homogenized with 0.1N $HNO_3$. The radioactivity of the buffer solution and homogenized oocytes was measured with a liquid scintillation counter (LIQUID SCINTILLATION SYSTEM; Aloka).

**LjMATE1 RNAi transformants of *L. japonicus***

For *LjMATE1* suppression by RNA interference, a 245 bp fragment (position 226-471) was amplified from the *LjMATE1* cDNA using a set of primers containing *att*B recombination sites for Gateway vector, forward primer, 5'-ACAAGTTTGTACAAAAAAGCAGGCTGGAGTTGCCATTGCTTTGTT -3'; reverse primer, 5'- ACCACTTTGTACAAGAAAGCTGGGTCTCAACACTTGCAGCCAAAA -3' (the underlines indicate specific sequences of the *att*B recombination sites). The PCR product was subcloned into pDONR/Zeo (Invitrogen), and then transferred into a Gateway-compatible binary vector, pUB-GWS-Hyg (Maekawa et al. 2008). The construct was used for plant transformation as described previously (Thykjaer et al. 1997). For phenotypic analysis, wild-type and T2 generation were grown either with supplementation of nitrogen nutrient

without rhizobia inoculation, or under nitrogen deficiency condition with rhizobia inoculation. Plants were sampled and photographed at 28 dpi. The nitrogenase activity was measured by the acetylene reduction assay (Maruya and Saeki 2010). For expression analysis of leghemoglobin, the set of primers specific to *leghemoglobin* was used (forward primer, 5'-TTTGAGCACTGCTTGGGGAGTAGCT-3' and reverse primer, 5'-AGGCATGCAAAACCAGAAAC-3'). The qPCR condition was described above. For hairy root transformation the RNAi fragment in pDONR/Zeo was transferred into a binary vector, pUB-GWS-GFP (Maekawa et al. 2008). The transformed hairy roots, selected with GFP signal, were inoculated with *M. loti* and sampled at 28 dpi.

**Perls staining**

For Perls staining, pink nodules were vacuum-infiltrated with equal volumes of 4% (v/v) HCl and 4% (w/v) K-ferrocyanide for 15 min, and incubated for 30 min at room temperature (Roschzttardtz et al. 2009). For the signal intensification with DAB and $H_2O_2$, the Perls stained nodules were fixed and embedded in Technovit 7100 as previously reported (Takanashi et al. 2012a). The sections (15 μm) were placed on glass slides, and then the intensification procedure was applied as described by Meguro et al. (Meguro et al. 2007).

**Measurement of the Fe content in nodules**

Seeds were germinated on a water agar plate. Five-day-old seedlings were transferred to sterile vermiculite with liquid 1/2 B&D medium in a plant box. After 2 days plants were inoculated by bacteria. At 28 dpi, the pink nodules were collected and dried in an oven at 70°C for 2 days.

Samples were then subjected to digestion with 0.5 ml of 61 % $HNO_3$ in a 2 ml plastic tube. The samples were heated up to 125°C for 5 hours and then diluted with 5% $HNO_3$. The metal concentration was determined by ICP-MS (7700X; Agilent Technologies).

**Funding**

This work was supported by the Japan Society for the Promotion of Science [Research Fellowships for Young Scientists (No. 09J00170 to K.T.), Grant-in-Aid for Scientific Research (No. 21027022 to K.Y.)].

**Acknowledgements**

We would like to thank National Bioresource Project (*Lotus japonicus*, *Glycine max*) for seeds of *L. japonicus* and pUB-GWS-GFP/Hyg, Dr. Tsuyoshi Nakagawa (Shimane University, Japan) for pGWB3, and Mrs. Make den Dulk-Ras (Leiden University, Netherland) for *A. rhizogenes* LBA1334.

**References**

Brewin, N.J. (1991) Development of the legume root nodule. *Annu. Rev. Cell Biol.* 7: 191-226.

Broughton, W.J. and Dilworth, M.J. (1971) Control of leghaemoglobin synthesis in snake beans. *Biochem. J.* 125: 1075-1080.

Colebatch, G., Desbrosses, G., Ott, T., Krusell, L., Montanari, O., Kloska, S., et al. (2004)

Global changes in transcription orchestrate metabolic differentiation during symbiotic nitrogen fixation in *Lotus japonicus*. *Plant J.* 39: 487-512.

Conte, S.S. and Walker, E.L. (2011) Transporters contributing to iron trafficking in plants. *Mol. Plant* 4: 464-476.

Delhaize, E., Gruber, B.D. and Ryan, P.R. (2007) The roles of organic anion permeases in aluminium resistance and mineral nutrition. *FEBS Lett.* 581: 2255-2262.

Durrett, T.P., Gassmann, W. and Rogers, E.E. (2007) The FRD3-mediated efflux of citrate into the root vasculature is necessary for efficient iron translocation. *Plant Physiol.* 144: 197-205.

Furukawa, J., Yamaji, N., Wang, H., Mitani, N., Murata, Y., Sato, K., et al. (2007) An aluminum-activated citrate transporter in barley. *Plant Cell Physiol.* 48: 1081-1091.

Green, L.S. and Rogers, E.E. (2004) FRD3 controls iron localization in Arabidopsis. *Plant Physiol.* 136: 2523-2531.

Hakoyama, T., Watanabe, H., Tomita, J., Yamamoto, A., Sato, S., Mori, Y., et al. (2009) Nicotianamine synthase specifically expressed in root nodules of *Lotus japonicus*. *Planta* 230: 309-317.

Ishimaru, Y., Masuda, H., Bashir, K., Inoue, H., Tsukamoto, T., Takahashi, M., et al. (2010) Rice metal-nicotianamine transporter, OsYSL2, is required for the long-distance transport of iron and manganese. *Plant J.* 62: 379-390.

Kaiser, B.N., Moreau, S., Castelli, J., Thomson, R., Lambert, A., Bogliolo, S., et al. (2003) The soybean NRAMP homologue, GmDMT1, is a symbiotic divalent metal transporter capable of ferrous iron transport. *Plant J.* 35: 295-304.

Kobayashi, T., Nakanishi, H. and Nishizawa, N.K. (2010) Recent insights into iron homeostasis and their application in graminaceous crops. *Proc. Jpn. Acad. Ser. B Phys. Biol. Sci.* 86: 900-913.

Kochian, L.V., Pineros, M.A. and Hoekenga, O.A. (2005) The physiology, genetics and molecular biology of plant aluminum resistance and toxicity. *Plant Soil* 274: 175-195.

Koike, S., Inoue, H., Mizuno, D., Takahashi, M., Nakanishi, H., Mori, S., et al. (2004) OsYSL2 is a rice metal-nicotianamine transporter that is regulated by iron and expressed in the phloem. *Plant J.* 39: 415-424.

Kouchi, H., Shimomura, K., Hata, S., Hirota, A., Wu, G.J., Kumagai, H., et al. (2004) Large-scale analysis of gene expression profiles during early stages of root nodule formation in a model legume, *Lotus japonicus*. *DNA Res.* 11: 263-274.

Krusell, L., Krause, K., Ott, T., Desbrosses, G., Kramer, U., Sato, S., et al. (2005) The sulfate transporter SST1 is crucial for symbiotic nitrogen fixation in *Lotus japonicus* root nodules. *Plant Cell* 17: 1625-1636.

Kumagai, H. and Kouchi, H. (2003) Gene silencing by expression of hairpin RNA in *Lotus japonicus* roots and root nodules. *Mol. Plant-Microbe Interact.* 16: 663-668.

LeVier, K., Day, D.A. and Guerinot, M.L. (1996) Iron uptake by symbiosomes from soybean root nodules. *Plant Physiol.* 111: 893-900.

Li, L.G., He, Z.Y., Pandey, G.K., Tsuchiya, T. and Luan, S. (2002) Functional cloning and characterization of a plant efflux carrier for multidrug and heavy metal detoxification. *J. Biol. Chem.* 277: 5360-5368.

Ma, J.F., Ryan, P.R. and Delhaize, E. (2001) Aluminium tolerance in plants and the complexing role of organic acids. *Trends Plant Sci.* 6: 273-278.

Ma, J.F., Tamai, K., Yamaji, N., Mitani, N., Konishi, S., Katsuhara, M., et al. (2006) A silicon transporter in rice. *Nature* 440: 688-691.

Maekawa, T., Kusakabe, M., Shimoda, Y., Sato, S., Tabata, S., Murooka, Y., et al. (2008)

Polyubiquitin promoter-based binary vectors for overexpression and gene silencing in *Lotus japonicus*. *Mol. Plant-Microbe Interact.* 21: 375-382.

Magalhaes, J.V., Liu, J., Guimaraes, C.T., Lana, U.G.P., Alves, V.M.C., Wang, Y.H., et al. (2007) A gene in the multidrug and toxic compound extrusion (MATE) family confers aluminum tolerance in sorghum. *Nat. Genet.* 39: 1156-1161.

Maruya, J. and Saeki, K. (2010) The *bacA* gene homolog, mlr7400, in *Mesorhizobium loti* MAFF303099 is dispensable for symbiosis with *Lotus japonicus* but partially capable of supporting the symbiotic function of *bacA* in *Sinorhizobium meliloti*. *Plant Cell Physiol.* 51: 1443-1452.

Meguro, R., Asano, Y., Odagiri, S., Li, C., Iwatsuki, H. and Shoumura, K. (2007) Nonheme-iron histochemistry for light and electron microscopy: a historical, theoretical and technical review. *Arch. Histol. Cytol.* 70: 1-19.

Moreau, S., Day, D.A. and Puppo, A. (1998) Ferrous iron is transported across the peribacteroid membrane of soybean nodules. *Planta* 207: 83-87.

Nakagawa, T., Kurose, T., Hino, T., Tanaka, K., Kawamukai, M., Niwa, Y., et al. (2007) Development of series of gateway binary vectors, pGWBs, for realizing efficient construction of fusion genes for plant transformation. *J. Biosci. Bioeng.* 104: 34-41.

Omote, H., Hiasa, M., Matsumoto, T., Otsuka, M. and Moriyama, Y. (2006) The MATE proteins as fundamental transporters of metabolic and xenobiotic organic cations. *Trends Pharmacol. Sci.* 27: 587-593.

Pelissier, H.C., Frerich, A., Desimone, M., Schumacher, K. and Tegeder, M. (2004) PvUPS1, an allantoin transporter in nodulated roots of French bean. *Plant Physiol.* 134: 664-675.

Price, G.D., Day, D.A. and Gresshoff, P.M. (1987) Rapid Isolation of Intact Peribacteroid Envelopes from Soybean Nodules and Demonstration of Selective Permeability to Metabolites. *J. Plant Physiol.* 130: 157-164.

Rogers, E.E., Wu, X.L., Stacey, G. and Nguyen, H.T. (2009) Two MATE proteins play a role in iron efficiency in soybean. *J. Plant Physiol.* 166: 1453-1459.

Roschzttardtz, H., Conejero, G., Curie, C. and Mari, S. (2009) Identification of the endodermal vacuole as the iron storage compartment in the Arabidopsis embryo. *Plant Physiol.* 151: 1329-1338.

Rosendahl, L., Vance, C.P. and Pedersen, W.B. (1990) Products of dark $CO_2$ Fixation in pea root nodules support bacteroid metabolism. *Plant Physiol.* 93: 12-19.

Smil, V. (1999) Nitrogen in crop production: an account of global flows. *Global Biogeochem. Cycle* 13: 647-662.

Takanashi, K., Sugiyama, A., Sato, S., Tabata, S. and Yazaki, K. (2012a) LjABCB1, an ATP-binding cassette protein specifically induced in uninfected cells of *Lotus japonicus* nodules. *J. Plant Physiol.* 169: 322-326.

Takanashi, K., Sugiyama, A. and Yazaki, K. (2011) Involvement of auxin distribution in root nodule development of *Lotus japonicus*. *Planta* 234: 73-81.

Takanashi, K., Takahashi, H., Sakurai, N., Sugiyama, A., Suzuki, H., Shibata, D., et al. (2012b) Tissue-specific transcriptome analysis in nodules of *Lotus japonicus*. *Mol. Plant-Microbe Interact.* 25: 869-876.

Tamura, K., Peterson, D., Peterson, N., Stecher, G., Nei, M. and Kumar, S. (2011) MEGA5: molecular evolutionary genetics analysis using maximum likelihood, evolutionary distance, and maximum parsimony methods. *Mol. Biol. Evol.* 28: 2731-2739.

Thykjaer, T., Finnemann, J., Schauser, L., Christensen, L., Poulsen, C. and Stougaard, J. (1997) Gene targeting approaches using positive-negative selection and large flanking regions. *Plant Mol. Biol.* 35: 523-530.

Uchiumi, T., Ohwada, T., Itakura, M., Mitsui, H., Nukui, N., Dawadi, P., et al. (2004) Expression islands clustered on the symbiosis island of the *Mesorhizobium loti* genome. *J. Bacteriol.* 186: 2439-2448.

Verma, D.P.S. and Hong, Z.L. (1996) Biogenesis of the peribacteroid membrane in root nodules. *Trends Microbiol.* 4: 364-368.

White, J., Prell, J., James, E.K. and Poole, P. (2007) Nutrient sharing between symbionts. *Plant Physiol.* 144: 604-614.

Wittenberg, J.B., Wittenberg, B.A., Day, D.A., Udvardi, M.K. and Appleby, C.A. (1996) Siderophore-bound iron in the peribacteroid space of soybean root nodules. *Plant Soil* 178: 161-169.

Yokosho, K., Yamaji, N. and Ma, J.F. (2010) Isolation and characterization of two MATE genes in rye. *Func. Plant Biol.* 37: 296–303.

Yokosho, K., Yamaji, N., Ueno, D., Mitani, N. and Ma, J.F. (2009) OsFRDL1 is a citrate transporter required for efficient translocation of iron in rice. *Plant Physiol.* 149: 297-305.

## Figure legends

**Fig. 1** Expression analyses of *LjMATE1*. (A) Tissue-specific semi-quantitative RT-PCR analysis of *LjMATE1*. (B) qPCR of *LjMATE1* in underground parts at different development stages of nodulation. Expression of *LjMATE1* was detected only in nodule, which increased at 7 dpi and kept high level of expression during nodulation. Values represent mean ± SD (n = 3). (C-H) GUS staining of *pLjMATE1*::GUS transformant. Whole nodules (C, E, G) and cross sections (D, F, H) of nodule at 7 (C, D), 21 (E, F), and 35 (G, H) dpi, respectively. Stained infected cells were found at 7 and 21 dpi (D, F). GUS expression mostly disappeared at 35 dpi (H). Bars = 200 μm.

**Fig. 2** An unrooted phylogenetic analysis of plant MATE transporters. Phylogenetic tree was generated using MEGA 5.0 software (Tamura et al. 2011). LjMATE1 and reported plant MATE transporter sequences were aligned using the ClustalW program. The neighbor-joining method was then used to construct a phylogenetic tree with 1,000 bootstrap replicates. MATE proteins in red were reported to be involved in Fe translocation or Al detoxification. Accession numbers and AGI codes are: AM1, FJ264202; AM3, FJ264203 (*Vitis vinifera*); AtALF5, At3g23560; AtDTX1, At2g04070; AtEDS5, At4g39030; AtFRD3, At3g08040; AtMATE, At1g51340; AtTT12, At3g59030; AtZRIZI, At1g58340 (*Arabidopsis thaliana*); GmFRD3a, EU591739; GmFRD3b, EU591741 (*Glycine max*); HvAACT1, AB302223 (*Hordeum vulgare*); LaMATE, AY631874 (*Lupinus albus*); MtMATE1, FJ858726; MtMATE2, HM856605 (*Medicago truncatula*); MTP77, Q6V7U8 (*Solanum lycopersicum*); NtJAT1, AM991692; NtMATE1, AB286961 (*Nicotiana tabacum*); OsFRDL1, Q10PY7 (*Oryza sativa*); SbMATE, EF611342

(*Sorghum bicolor*); ScFRDL1, AB571881; ScFRDL2, AB571882 (*Secale cereale*); ZmMATE1, FJ015155 (*Zea mays*).

**Fig. 3** Transport activity of LjMATE1 measured in *Xenopus* oocytes. The LjMATE1-expressing oocytes were injected with $^{14}$C-labeled citrate or $^{14}$C-malate and their release from the oocytes was determined 30 min after injection. LjMATE1 showed an efflux activity for citrate, but not for malate. Values represent mean ± SD (n = 4). *$p$<0.01 compared with control ($H_2O$) by Student's t-test.

**Fig. 4** Phenotype of 5-week-old *LjMATE1* RNAi knock-down lines. Plants were grown in vermiculite with (+N) or without (-N) nitrogen supplementation. (A) Expression analysis of *LjMATE1* in RNAi lines with qPCR. Values represent mean ± SD (n = 3). (B) Shoot length of control and RNAi lines under nitrogen deficiency condition. Values represent mean ± SD (n = 16). (C) Growth phenotype of 5-week-old rhizobia-inoculated plant (28 dpi). Growth of *ljmate1* was clearly suppressed under nitrogen deficiency condition. Scale bar = 2 cm. (A, B) *$p$<0.01 compared with controls by Tukey-Kramer test.

**Fig. 5** Phenotype of *L. japonicus* nodules at 28 dpi. Nodule phenotype (A, WT; B, *ljmate1*; C, *LjMATE1*), number per plant (D, n = 10-18), size (E, n = 19-31), and ARA (F, n = 32-55) of wild-type and RNAi lines. (G) Expression level of leghemoglobin in nodules (n = 3). In *ljmate1* greenish nodules were observed as well as pink nodules, and reduced nitrogen fixation activity was measured. Scale bars = 1 mm. Values represent mean ± SD. *$p$<0.05, **$p$<0.01 compared

to controls by Tukey-Kramer test.

**Fig. 6** Fe accumulation in nodules was examined with Perls staining. Fe precipitation was not observed inside wild-type nodules from either top (A) or nodule-root junction (B) side. In *ljmate1* Fe accumulation was not seen from the nodule top side (C), while strong blue staining was detected at nodule-root junction (D, pointed by arrowhead) and nodule vascular bundle. In *LjMATE1* the blue staining was not observed at both top (E) and nodule-root junction (F) side. Scale bars = 200 μm.

**Fig. 7** Typical Fe localization inside the nodules of wild-type (A-C), *ljmate1* (D-F) and *LjMATE1* (G-I). Perls staining was enhanced by DAB and $H_2O_2$. (A, B) High Fe accumulation was observed in infected cells in wild-type nodule. (C) Root vascular bundle was not stained in wild-type. (D, E) Fe accumulation in infection zone was reduced in *ljmate1*, especially in the central region. (F) Abnormality in the Fe accumulation was also detected in root vascular bundle. (G-I) Same Fe accumulation pattern was observed in *LjMATE1* nodule with wild-type. (A, D, G) Root vascular bundle was pointed by arrowheads. Scale bars = 100 μm.

**Fig. 8** Fe and other metal contents in *L. japonicus* nodules determined by ICP-MS. The nodules of wild-type and *ljmate1* plants were sampled at 28 dpi. The Fe concentration of *ljmate1* was reduced to 56.8% of WT. Values represent mean ± SD (n = 3). *$p$<0.05 compared with WT by Student's t-test.

Fig. 1

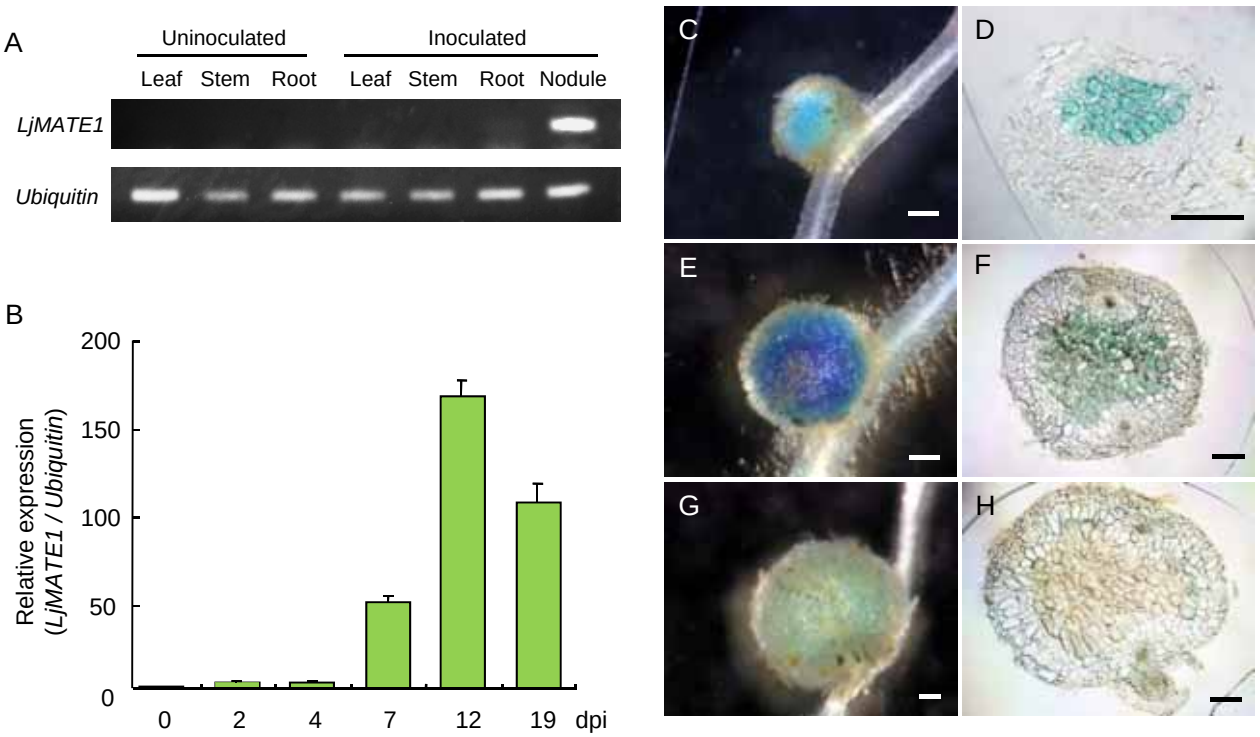
A
Uninoculated
Inoculated
Leaf
Stem
Root
Leaf
Stem
Root
Nodule
LjMATE1
Ubiquitin
B
Relative expression
(LjMATE1 / Ubiquitin)
200
150
100
50
0
0
2
4
7
12
19
dpi
C
D
E
F
G
H

Fig. 2

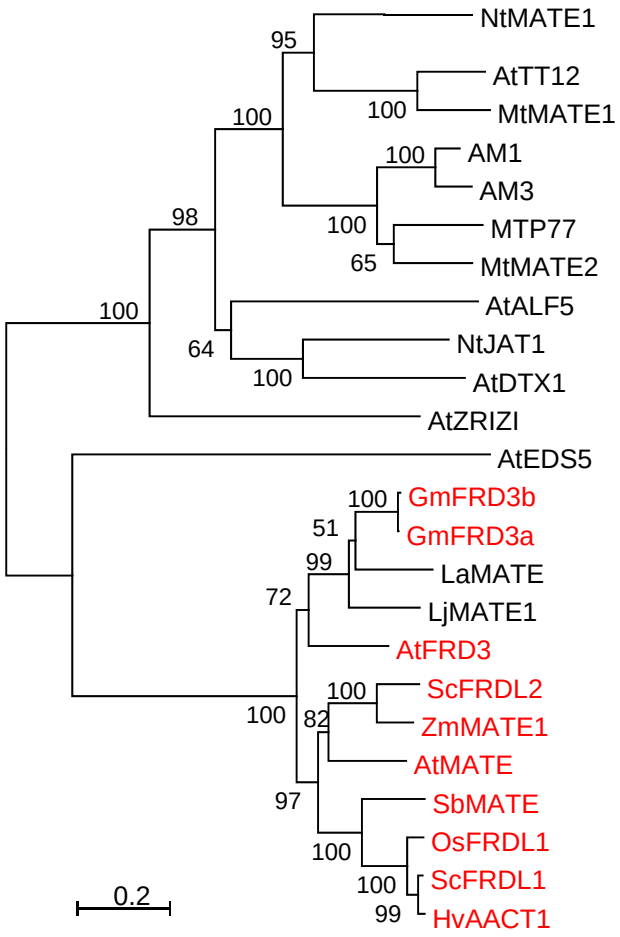
NtMATE1
AtTT12
MtMATE1
AM1
AM3
MTP77
MtMATE2
AtALF5
NtJAT1
AtDTX1
AtZRIZI
AtEDS5
GmFRD3b
GmFRD3a
LaMATE
LjMATE1
AtFRD3
ScFRDL2
ZmMATE1
AtMATE
SbMATE
OsFRDL1
ScFRDL1
HvAACT1
95
100
100
100
98
100
65
100
64
100
100
51
99
72
100
82
97
100
100
99
0.2

Fig. 3

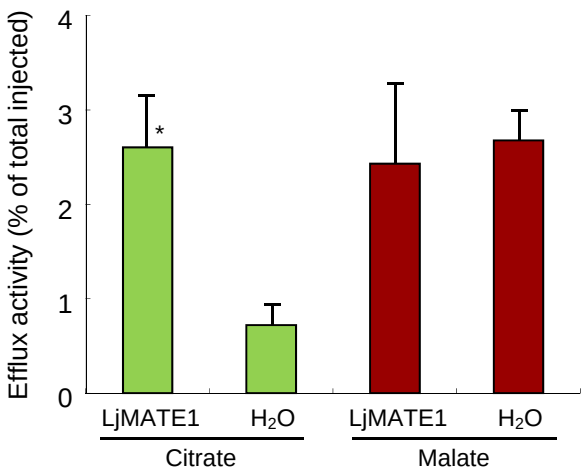
Efflux activity (% of total injected)
4
3
2
1
0
*
LjMATE1
H2O
LjMATE1
H2O
Citrate
Malate

Fig. 4

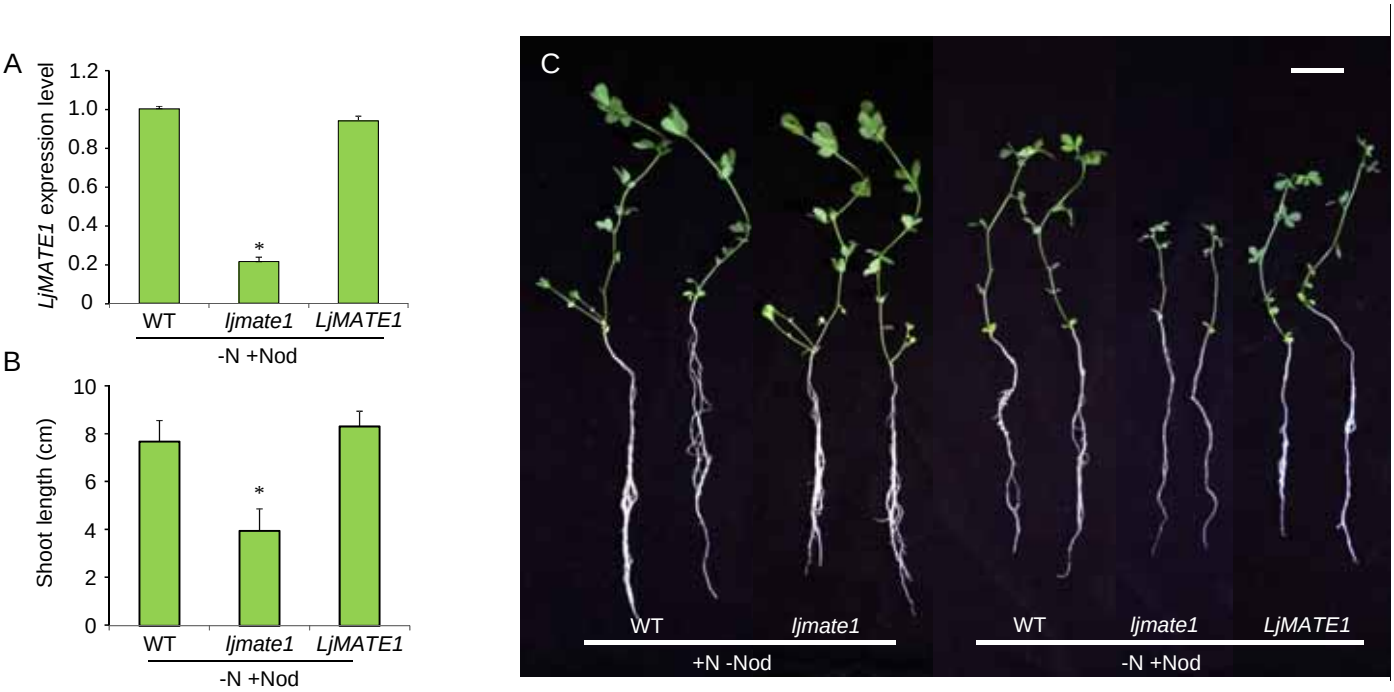
A
LjMATE1 expression level
1.2
1.0
0.8
0.6
0.4
0.2
0
*
WT
ljmate1
LjMATE1
-N +Nod
B
Shoot length (cm)
10
8
6
4
2
0
*
WT
ljmate1
LjMATE1
-N +Nod
C
WT
ljmate1
+N -Nod
WT
ljmate1
LjMATE1
-N +Nod

Fig. 5

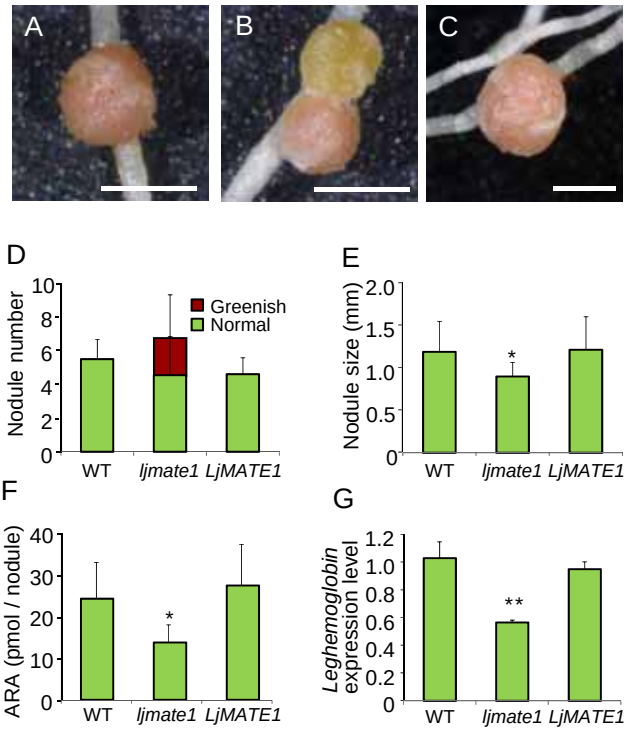
A
B
C
D
Nodule number
Greenish
Normal
WT
ljmate1
LjMATE1
E
Nodule size (mm)
F
ARA (pmol / nodule)
G
Leghemoglobin expression level

Fig. 6

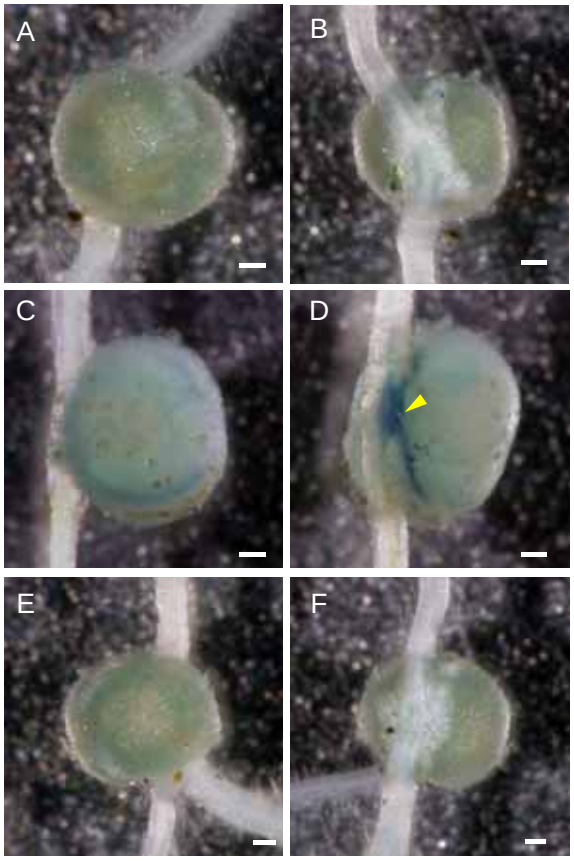

Fig. 7

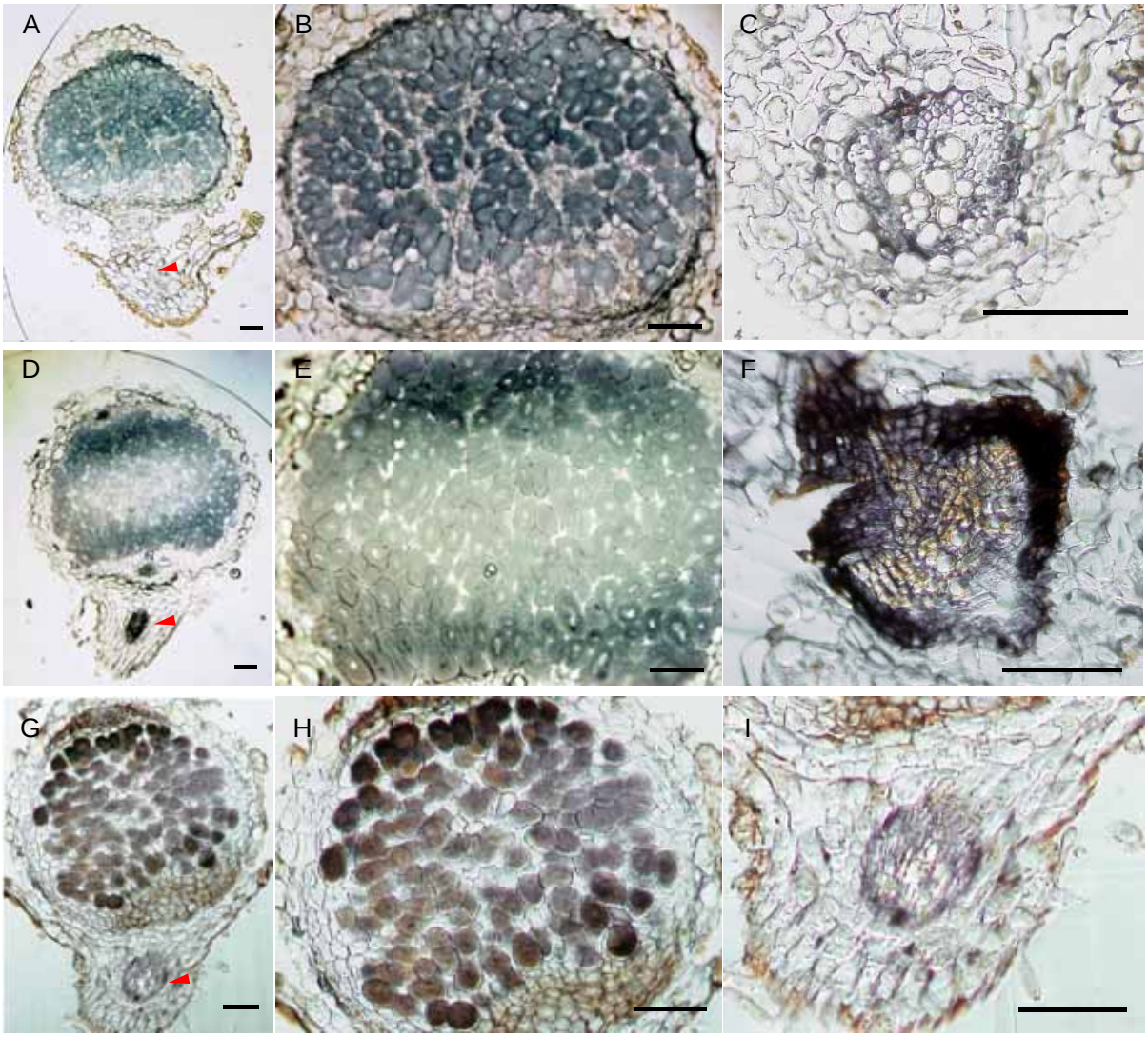

Fig. 8

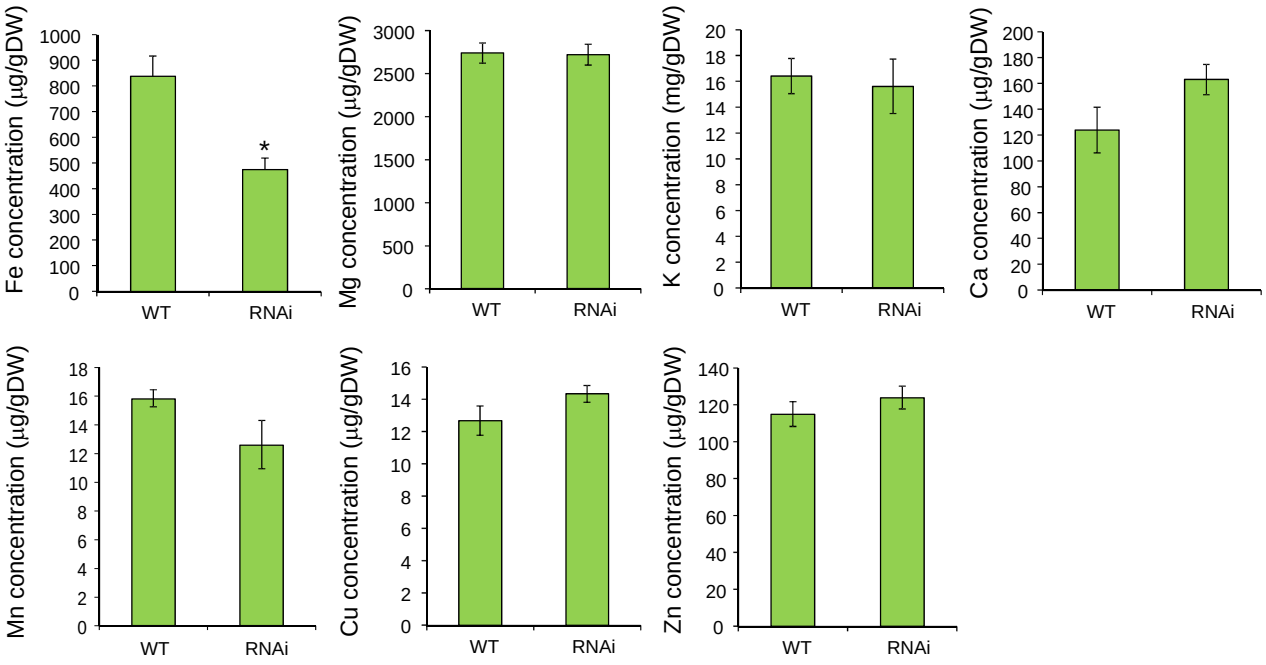
Fe concentration (μg/gDW)
1000
900
800
700
600
500
400
300
200
100
0
*
WT
RNAi
Mg concentration (μg/gDW)
3000
2500
2000
1500
1000
500
0
WT
RNAi
K concentration (mg/gDW)
20
18
16
14
12
10
8
6
4
2
0
WT
RNAi
Ca concentration (μg/gDW)
200
180
160
140
120
100
80
60
40
20
0
WT
RNAi
Mn concentration (μg/gDW)
18
16
14
12
10
8
6
4
2
0
WT
RNAi
Cu concentration (μg/gDW)
16
14
12
10
8
6
4
2
0
WT
RNAi
Zn concentration (μg/gDW)
140
120
100
80
60
40
20
0
WT
RNAi

# Supplementary Fig. S1

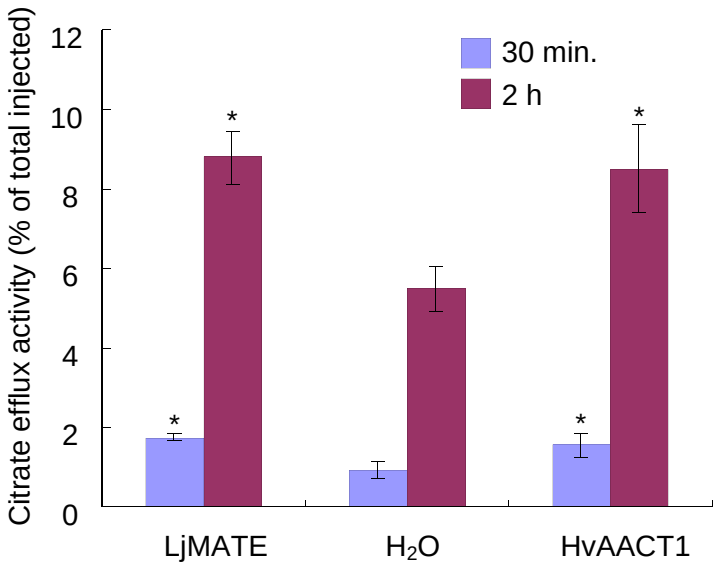


**Citrate transport activity of LjMATE1 and HvAACT1 measured in *Xenopus* oocytes.** The oocytes were injected with $^{14}$C-labeled citrate, and their release from the oocytes was determined 30 min and 2 h after injection. LjMATE1 showed same efflux activity for citrate with HvAACT1. Values represent mean ± SD (n = 3-4). *$p$<0.01 compared to control ($H_2O$) by Tukey-Kramer test.

Supplementary Fig. S2

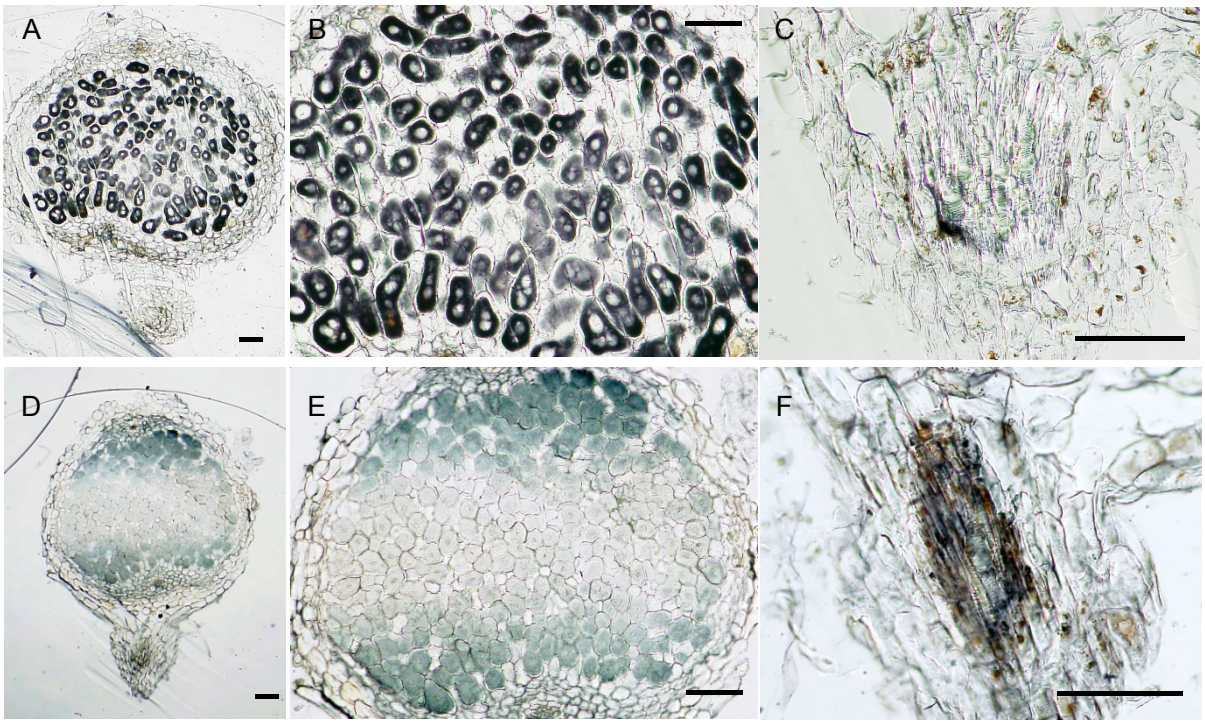


**Typical Fe localization inside the nodules of control (A-C) and hairy root RNAi (D-F).** Perls staining was enhanced by DAB and $H_2O_2$. (A, B) High Fe accumulation was observed in infected cells in control nodule. (C) Root vascular bundle was not stained in control. (D, E) Fe accumulation in infection zone was reduced in RNAi, especially in the central region. (F) Abnormality in the Fe accumulation was also detected in root vascular bundle. Scale bars = 100 mm.